

Dalton Transactions

An international journal of inorganic chemistry

Accepted Manuscript

This article can be cited before page numbers have been issued, to do this please use: V. H. Araujo Pinto, N. K. S. M. Falcao, B. Mariz-Silva, M. G. Fonseca and J. S. Reboucas, *Dalton Trans.*, 2020, DOI: 10.1039/D0DT01383H.



This is an Accepted Manuscript, which has been through the Royal Society of Chemistry peer review process and has been accepted for publication.

Accepted Manuscripts are published online shortly after acceptance, before technical editing, formatting and proof reading. Using this free service, authors can make their results available to the community, in citable form, before we publish the edited article. We will replace this Accepted Manuscript with the edited and formatted Advance Article as soon as it is available.

You can find more information about Accepted Manuscripts in the [Information for Authors](#).

Please note that technical editing may introduce minor changes to the text and/or graphics, which may alter content. The journal's standard [Terms & Conditions](#) and the [Ethical guidelines](#) still apply. In no event shall the Royal Society of Chemistry be held responsible for any errors or omissions in this Accepted Manuscript or any consequences arising from the use of any information it contains.

1 **Robust Mn(III) *N*-pyridylporphyrin-based biomimetic catalysts for**
2 **hydrocarbon oxidations: Heterogenization on non-functionalized silica gel**
3 **versus chloropropyl-functionalized silica gel**
4
5
6
7

8 Victor Hugo A. Pinto, Nathália K. S. M. Falcão, Bárbara Mariz-Silva, Maria
9 Gardennia da Fonseca, Júlio S. Rebouças*

10
11
12
13
14 Department of Chemistry, CCEN, Universidade Federal da Paraíba, João
15 Pessoa, PB, 58051-900, Brazil.

16
17
18
19
20 *Author for correspondence: Dr. Júlio Santos Rebouças, Universidade Federal
21 da Paraíba, Departamento de Química, João Pessoa/PB, 58051-900, Brazil,
22 Tel./Fax: +55-83-3216-7591, E-mail address: jsreboucas@quimica.ufpb.br (Júlio
23 S. Rebouças); ORCID: 0000-0003-3818-029X
24

25 Abstract

View Article Online
DOI: 10.1039/D0DT01383H

26 Two classes of heterogenized biomimetic catalysts were prepared and
27 characterized for hydrocarbon oxidations: (1) by covalent anchorage of the three
28 Mn(III) *meso*-tetrakis(2-, 3-, or 4-pyridyl)porphyrin isomers by in situ alkylation
29 with chloropropyl-functionalized silica gel (**Sil-CI**) to yield **Sil-CI/MnPY** (**Y = 1, 2,**
30 **3**) materials, and (2) by electrostatic immobilization of the three Mn(III) *meso*-
31 tetrakis(*N*-methylpyridinium-2, 3, or 4-yl)porphyrin isomers (**MnPY**, **Y = 4, 5, 6**)
32 on non-modified silica gel (**SiO₂**) to yield **SiO₂/MnPY** (**Y = 4, 5, 6**) materials. Silica
33 gel used was of column chromatography grade and Mn porphyrin loadings were
34 deliberately kept at a low level (0.3% w/w). These resulting materials were
35 explored as catalysts for iodosylbenzene (PhIO) oxidation of cyclohexane, *n*-
36 heptane, and adamantane to yield the corresponding alcohols and ketones; the
37 oxidation of cyclohexanol to cyclohexanone was also investigated. The
38 heterogenized catalysts exhibited higher efficiency and selectivity than the
39 corresponding Mn porphyrins under homogeneous conditions. Recycling studies
40 were consistent with low leaching/destruction of the supported Mn porphyrins.
41 The **Sil-CI/MnPY** catalysts were more efficient and more selective than
42 **SiO₂/MnPY** ones; alcohol selectivity may be associated with hydrophobic silica
43 surface modification reminiscent of biological cytochrome P450 oxidations. The
44 use of widespread, column chromatography, amorphous silica yielded **Sil-**
45 **CI/MnPY** or **SiO₂/MnPY** catalysts considerably more efficient than the
46 corresponding, previously reported materials with mesoporous Santa Barbara
47 Amorphous No 15 (SBA-15) silica. Among the materials studied, in situ
48 derivatization of Mn(III) 2-*N*-pyridylporphyrin by covalent immobilization on **Sil-CI**
49 to yield **Sil-CI/MnP1** showed the best catalytic performance with high stability
50 against oxidative destruction and reusability/recycle.

51

52

53 **Keywords:** porphyrin, silica gel, immobilization, oxyfunctionalization, alkane,
54 biomimetic catalysis

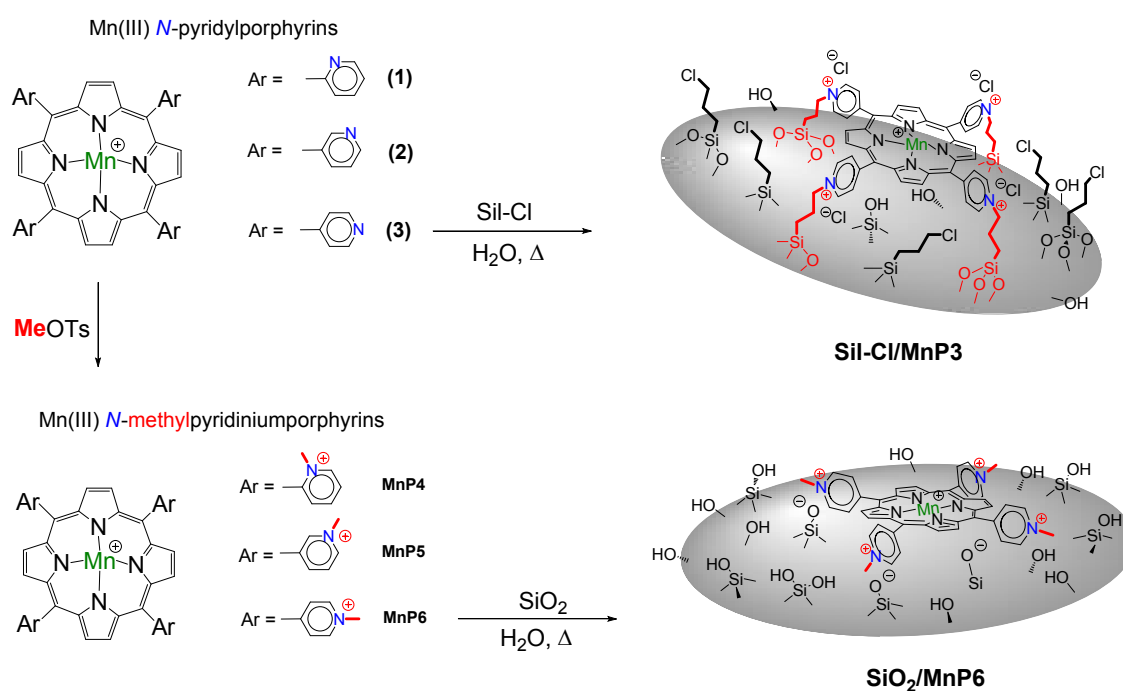
55

56 Abbreviations

57 MnP, Mn porphyrin; MnPs, Mn porphyrins; CPTS, (3-chloropropyl)trimethoxysilane;
58 Sil-Cl, 3-chloropropyl-functionalized silica gel; **(1)**, Mn(III) *meso*-tetrakis(2-
59 pyridyl)porphyrin chloride (also known in the literature as MnT-2-PyPCI); **(2)**,
60 Mn(III) *meso*-tetrakis(3-pyridyl)porphyrin chloride (also known in the literature as
61 MnT-3-PyPCI), **(3)**, Mn(III) *meso*-tetrakis(4-pyridyl)porphyrin chloride (also known
62 in the literature as MnT-4-PyPCI); MnP4, Mn(III) *meso*-tetrakis(*N*-
63 methylpyridinium-2-yl)porphyrin chloride (also known in the literature as MnTM-
64 2-PyPCl₅); MnP5, Mn(III) *meso*-tetrakis(*N*-methylpyridinium-3-yl)porphyrin
65 chloride (also known in the literature as MnTM-3-PyPCl₅); MnP6, Mn(III) *meso*-
66 tetrakis(*N*-methylpyridinium-4-yl)porphyrin chloride (also known in the literature
67 as MnTM-4-PyPCl₅); MCM-41, mesoporous silica Mobil Composition Matter No
68 41; SBA-15, mesoporous silica Santa Barbara Amorphous No 15; DR-UV/VIS,
69 diffuse reflectance UV/VIS spectroscopy; Cy-H, cyclohexane; Cy-ol,
70 cyclohexanol; Cy-one, cyclohexanone; Adm, adamantane; Adm-1-ol, 1-
71 adamantanol; Adm-2-ol, 2-adamantanol; 1-ol, 1-heptanol; 2-ol, 2-heptanol; 3-ol,
72 3-heptanol; 4-ol, 4-heptanol; 2-one, 2-heptanone; 3-one, 3-heptanone; 4-one, 4-
73 heptanone.

1 Introduction

2 The three neutral Mn(III) *meso*-tetrakis(2-, 3-, or 4-pyridyl)porphyrin
 3 isomers [(**1**), (**2**), (**3**)] and their three methylated, cationic derivatives Mn(III)
 4 *meso*-tetrakis(*N*-methylpyridinium-2, 3, or 4-yl)porphyrins (**MnPY**, **Y** = **4**, **5**, **6**)
 5 (Fig. 1) comprise a class of Mn porphyrins (MnPs) greatly studied as biomimetic
 6 models for oxidoreductase enzymes, such as, cytochromes P450, peroxidases,
 7 catalases, and superoxide dismutases, under homogeneous conditions.¹⁻¹¹
 8 Although these Mn porphyrins possess structural features, such as dangling
 9 pyridyl moieties on (**1**), (**2**), and (**3**) (suited for quaternization reactions) or
 10 permanent cationic *N*-methylpyridinium moieties on **MnPY** (**Y** = **4**, **5**, **6**) (suited
 11 for electrostatic interactions), they remain little explored as heterogenized
 12 oxidation catalysts as compared to regular *meso*-tetraphenylporphyrin
 13 derivatives.^{12,13} Among the isomers of these Mn porphyrins, most of the
 14 heterogenization work is centered on (**3**) and **MnP6**, given their traditionally
 15 easier preparation routes and commercial availability.



17

18 **Figure 1.** Schematic representation of the two classes of catalysts prepared and
 19 used in this work: in situ derivatization of neutral Mn porphyrin (**3**) by 3-
 20 chloropropyl-functionalized silica gel (**Sil-Cl**) to yield **Sil-Cl/MnP3** (related (**1**) and
 21 (**2**) isomers were anchored similarly); methyl tosylate (MeOTs) derivatization of
 22 (**3**) to yield cationic Mn porphyrin **MnP6** followed by immobilization on **silica gel**

23 (**SiO₂**) to yield **SiO₂/MnP6** (related **MnP4** and **MnP5** isomers were anchored
24 similarly). View Article Online
DOI: 10.1039/D0DT01383H

25

26 Neutral Mn(III) *meso*-tetrakis(2-, 3-, or 4-pyridyl)porphyrins (**(1)**, **(2)**, **(3)**) are
27 simple first-generation Mn porphyrins amenable to immobilization on haloalkane-
28 functionalized materials through covalent bonding between the porphyrin pyridyl
29 moieties and the support-based pendant organic halides, generating a cationic
30 *N*-alkylpyridinium moiety of a **MnPY**-type structure with halide as counter-
31 ion.^{1,14,15} Thus, **(3)** has been successfully anchored on iodopropyl- and
32 chloropropyl-functionalized silica gel (Sil-I and Sil-Cl, respectively)^{14,15} or
33 chloropropyl silica-coated magnetic nanoparticles¹⁶ for alkene epoxidations and
34 alkane hydroxylations. **(3)** supported on chloromethylated polystyrene yielded
35 suitable catalysts for alkene epoxidation, alkane oxidation, sulfides oxidation, and
36 carboxylic acid decarboxylation.¹⁷⁻¹⁹ Of note, the Fe(III) analogue of **(3)** was
37 immobilized on Sil-Cl and chloropropyl-functionalized Santa Barbara Amorphous
38 No 15 mesoporous silica (SBA-15Cl) for the oxidative degradation of
39 pentabromophenol.²⁰

40 Mn(III) *N*-methylpyridiniumporphyrins (**MnPY**, **Y = 4, 5, 6**) are the simplest
41 second-generation Mn porphyrins derived from **(1)**, **(2)**, and **(3)**, respectively (Fig.
42 1). They are a class of water-soluble cationic MnPs considerably more studied in
43 catalysis than their neutral precursors **(1)**, **(2)**, **(3)**. Their immobilization on inert
44 supports may be readily achieved by electrostatic interactions between the **MnPY**
45 permanent positive pyridinium charges and a negative support surface.^{3,12,21}
46 **MnPY**-based oxidative heterogenized catalysts have been prepared by
47 anchoring these cationic MnPs on supports, such as, non-modified amorphous
48 silica gel,^{12,22} imidazole- or sulfonato-functionalized amorphous silica²³, Mobil
49 Composition Matter No 41 (MCM-41) and Santa Barbara Amorphous No 15
50 (SBA-15) mesoporous silica,^{1,3,24} amorphous- or hexagonal mesoporous silica
51 (HMS)-coated magnetic nanoparticles,^{3,25} and clays.^{21,26} As compared to the
52 corresponding homogenous systems, heterogenization of **MnP6** yielded
53 generally better oxidation catalysts.^{12,24,26}

54 Recently, a joint effort between our group and Nakagaki's group¹ resulted
55 in 2 classes of mesoporous SBA-15-based materials exploiting these Mn
56 porphyrins, i.e., **(1)**, **(2)**, and **(3)**, covalently derivatized by and heterogenized on

57 chloropropyl-functionalized mesoporous SBA-15 silica (**SBA-15Cl/MnPY**) and
58 **MnPY** isomers electrostatically immobilized on non-functionalized mesoporous
59 SBA-15 silica (**SBA-15/MnPY**). These materials were able to catalyze the
60 cyclohexane (Cy-H) oxidation to cyclohexanol (Cy-ol) and cyclohexanone (Cy-
61 one) by iodobenzene (PhIO) with moderate yields, good selectivity toward
62 alcohol, and excellent recyclability. Cyclohexane and cyclohexanol are well-
63 studied substrates for model oxidation reactions and of industrial and economic
64 relevance²⁷⁻³⁰ to the production of adipic acid and caprolactam, which are, in turn,
65 used for the manufacture of nylons (nylon-66 and nylon-6).²⁷⁻²⁹

66 Herein we simplified and extended the scope of these heterogenized
67 catalytic systems by replacing SBA-15-type silicas with cheaper, ordinary,
68 column chromatography grade, amorphous silica gel as inert supports, to yield
69 the corresponding classes of materials containing covalently bound cationic
70 complexes (**Sil-Cl/MnPY**, **Y = 1, 2, 3**) and electrostatically immobilized cationic
71 **MnPY** complexes (**SiO₂/MnPY**, **Y = 4, 5, 6**) (Fig. 1). Given the low cost and
72 widespread availability of chromatographic silica in chemistry laboratories, these
73 new **Sil-Cl/MnPY** and **SiO₂/MnPY** materials should be of broader interest and
74 greater accessibility for oxidation catalysis than our previously reported SBA-15-
75 based systems. Neutral (**1**), (**2**), and (**3**) and cationic MnPYs are the Mn porphyrin
76 sources for the preparation of these heterogenized catalysts. Despite their
77 different chemical nature prior to immobilization, the final porphyrinoid
78 compounds supported on both Sil-Cl and SiO₂ surfaces are all MnPY-type,
79 cationic Mn(III) *N*-alkylpyridylporphyrins (**Sil-Cl/MnPY** and **SiO₂/MnPY**, Fig. 1).

80 All six solids were investigated as catalysts for PhIO-oxidation of cyclic
81 alkanes (cyclohexane and adamantane) and a linear alkane (n-heptane). The
82 oxidation of cyclohexanol to cyclohexanone was also investigated as a control
83 reaction. The impact of the materials on catalytic efficiency, selectivity, and
84 recyclability were also addressed with respect to: 1) the effect of MnP
85 heterogenization (vs. homogenous systems); 2) the nature of the immobilized Mn
86 porphyrin isomers, 3) catalyst oxidative stability; and 4) some hints on the effects
87 of the support (**SiO₂** vs. **Sil-Cl**). Additionally, direct comparisons on the Cy-H
88 oxidation data with the corresponding literature mesoporous SBA-15 silica
89 systems¹ were undertaken.

90

91 Experimental

92 General Information

93 All reagents and solvents were of commercial, high purity grade and
94 detailed in the Electronic Supplementary Information (ESI, Section S1). Silica gel
95 for column chromatography (**SiO₂**, high-purity grade, particle size of 70 230
96 mesh, median pore diameter 60 Å, Aldrich) was activated as described
97 elsewhere.³¹ **Sil-CI** was prepared using a slightly modified literature procedure³²
98 and characterized^{3,12,16-23,25,26,31,33-36} as described in ESI (Sections S2 and S3).
99 Complexes **(1)**, **(2)**, **(3)**, and **MnPY (Y = 4, 5, 6)** were prepared by literature
100 routes.^{4,37,38-40} The isolated complexes in the chloride form were
101 chromatographically and spectroscopically identical to the samples used in our
102 previous study¹ to those reported elsewhere.^{4,5,41,38,42-44} Tosylate (OTs⁻) salts of
103 **MnPY (Y = 4, 5, 6)** were prepared by ion exchange chromatography.⁴⁵ Details on
104 MnP synthesis and characterization are given in ESI (Section S4 and S5).
105 Iodosylbenzene (PhIO) was prepared from (diacetoxyiodo)benzene (PhI(OAc)₂,
106 Aldrich) as reported elsewhere.⁴⁶ PhIO was stored under refrigeration and its
107 active oxygen content was determined periodically by iodometry. All equipment
108 for analytical and physical measurements are given in ESI (Section S1).

109

110 Preparation of **Sil-CI/MnPY (Y = 1, 2, 3)** materials

111 The detailed preparations of these materials are given in ESI (Section S6).
112 Briefly, 19.55 μmol of **(1)** (as a 0.405 mmol L⁻¹ aqueous solution) and 5.00 g of
113 **Sil-CI** were refluxed under mechanical stirring for 24 h until a full discoloration of
114 the supernatant and a darkening of the solids were observed. The suspension
115 was filtered and the solid was washed with small portions of H₂O until the
116 presence of MnP in the washings was not detected by UV/VIS spectroscopy; the
117 washing procedure was repeated with MeOH, EtOH, and CHCl₃ (in this order).
118 All washings were collected to allow for the spectrophotometric determination of
119 non-immobilized **(1)**. The resulting solid was oven dried at 80 °C for 24 h to yield
120 4.86 g of **Sil-CI/MnP1** as a light orange material. The amount of Mn porphyrin
121 immobilized onto **Sil-CI** was determined indirectly by analyzing
122 spectrophotometrically the recovered Mn porphyrin in reaction supernatant and
123 washing solutions as reported elsewhere.¹⁻³ Mn porphyrin loading (in μmol MnP

per g of **SiI-CI**) was calculated as the ratio between the immobilized amount of MnP and the starting mass of **SiI-CI**. The immobilization yield was defined as the ratio between the amounts of immobilized versus starting MnP. Preparations of **SiI-CI/MnP2** and **SiI-CI/MnP3** as light green solids were carried out similarly (see ESI, Section S6 for details).

These reactions were repeated by different coauthors, using independently prepared samples, to check for reproducibility. No apparent differences were observed between corresponding **SiI-CI/MnP_Y** (**Y = 1, 2, 3**) batches.

Preparation of **SiO₂/MnP_Y** (**Y = 4, 5, 6**) materials

The synthesis and workup procedures for the electrostatic heterogenization of the chloride salts of cationic **MnP_Y** isomers (**Y = 4, 5, 6**) onto **SiO₂** were similar to that described for the **SiI-CI/MnP_Y** materials, except that the nature of the starting reagents were changed and the reaction time was shortened to 3 h (see ESI, Section S7, for details). MnPY loadings and immobilization yields were determined as described above.

Oxidation reactions

A detailed description of the methodology used for the oxidation reactions is given in ESI (Sections S8 and S9). Briefly, 2 mL vials were charged with predefined amounts of PhIO, catalyst, 1:1 MeCN:CHCl₃ solvent, and substrate, and sealed with a teflon/silicone septum and a screw cap. The oxidation reactions were carried out at room temperature (*ca.* 26 °C), under air, in the absence of light, with magnetic stirring. The reactions were quenched at 90 min with 50 μL of a saturated sodium tetraborate and sodium sulfite aqueous solution (see ESI, Section S9). Then, 50 μL of a 28 mmol L⁻¹ solution of a GC internal standard in MeCN:CHCl₃ (1:1, v/v) was added. The products of the reactions were quantified by gas chromatography (GC). Bromobenzene (PhBr) was used as internal standard for the reactions with cyclohexane, cyclohexanol, and adamantane as substrates, while 1-octanol was used in the reactions of n-heptane oxidation. The reported yields for all products represent an average of least three replicates and were calculated based on the initial amount of PhIO (limiting reactant), considering the following stoichiometry: 1 mol of PhIO per mol of alcohol and 2

158 mols of PhIO per mol of aldehyde or ketones.^{1,4,12} For the homogeneous systems
159 (using non-immobilized MnP), MnP destruction (bleaching) was determined
160 spectrophotometrically after quenching the reaction.

161 For the recycling studies, the solid catalysts were recovered by
162 centrifugation, washed with CHCl₃, EtOH, MeOH, and H₂O (in this order), dried
163 at 80 °C for 6 h, and, then, reused in a new oxidation run. The reaction media
164 and collected washings were analyzed by UV/VIS spectroscopy to verify whether
165 there was leaching of MnPs from the solid catalysts.

166 The control reactions were carried out in the absence of catalysts but
167 containing (i) PhIO+substrate+solvent, (ii) support+substrate+solvent (labeled
168 **SiI-Cl** or **SiO₂** entries), (iii) supports+PhIO+substrate+solvent (labeled **SiO₂/PhIO**
169 or **SiI-Cl/PhIO** entries).

170

171

172 Results and discussion

173 Characterization of SiI-Cl and SiO₂ supports

174 **SiI-Cl** was synthesized by chemical functionalization of chromatographic
175 grade amorphous silica gel (**SiO₂**) with CPTS by the heterogeneous route.³² The
176 amount of chloropropyl moieties on the silica surface was estimated by elemental
177 analysis of carbon (3.72%) and chlorine (2.91%), which is consistent with a
178 functionalization of 930 μmol g⁻¹, considering the a stoichiometry of three carbon
179 atoms per chlorine atom. Both **SiI-Cl** and **SiO₂** were also characterized by fourier-
180 transform infrared spectroscopy, thermogravimetric analysis, textural analyses,
181 scanning electron microscopy, transmission electron microscopy, and ²⁹Si and
182 ¹³C nuclear magnetic resonance spectroscopies. The results agree with literature
183 data and the corresponding discussions are presented in ESI (Section S3).

184

185 Preparation of SiI-Cl/MnPY (Y = 1, 2, 3) and SiO₂/MnPY (Y = 4, 5, 6).

186 Two classes of heterogenized catalysts were prepared either by in situ
187 derivatization and covalent immobilization of **(1)**, **(2)**, or **(3)** on **SiI-Cl** to yield
188 **SiI-Cl/MnPY** catalysts (Fig. 1), or by electrostatic immobilization of **MnPY (Y = 4,**
189 **5, 6)** on **SiO₂** to yield **SiO₂/MnPY** catalysts (Fig. 1). The immobilization of MnPX
190 on SiI-Cl explores the quaternization of the *N*-pyridyl moieties of MnPX directly

191 by the surface chloropropyl groups of Sil-Cl, mimicking, thus, a regular, organic
 192 halide-based alkylating agent (Fig. 1). Conversely, for the immobilization process
 193 of MnPY onto SiO₂, MnPX was initially quaternized *via* *N*-pyridyl methylation to
 194 yield MnPY,^{38,40} which was then immobilized onto SiO₂ by exploring the cationic
 195 nature of the MnPY *N*-methylpyridinium moieties and the anionic nature of SiO₂
 196 surface.^{1,2,12,13}

197 The MnP immobilization yields and the MnP loadings on **Sil-Cl/MnPY (Y**
 198 **= 1, 2, 3)** and **SiO₂/MnPY (Y = 4, 5, 6)** were calculated by the difference between
 199 the initial amount of MnP used in the reaction and the amount of unreacted MnP
 200 recovered in the reaction supernatant and washings (Table 1). The amount of
 201 unreacted, recovered MnP in the various washings was determined
 202 spectrophotometrically, as in related systems.¹⁻³ Attempts to quantify MnP in the
 203 solids by UV/VIS (by destroying the silica matrix with aqueous NaOH) or directly
 204 by diffuse reflectance UV/VIS (DR-UV/VIS) were unsuccessful. Attempts to
 205 quantify Mn content by atomic absorption spectroscopy gave unreliable results in
 206 our hands so far, most likely due to unoptimized method for sample treatment.

207

208 **Table 1.** Isolation yields, MnP immobilization yields and MnP loadings related to
 209 the **Sil-Cl/MnPY (Y = 1, 2, 3)** and **SiO₂/MnPY (Y = 4, 5, 6)** solids.

Solids	Isolation yield /%	Immobilization yield /% ^a	MnP Loading / $\mu\text{mol g}^{-1}$ ^a
Sil-Cl/MnP1	97	92±5	4.3±0.9
Sil-Cl/MnP2	98	90±3	4.1±0.1
Sil-Cl/MnP3	98	97±2	5.9±0.9
SiO ₂ /MnP4	~100	~100	5.2
SiO ₂ /MnP5	~100	~100	4.6
SiO ₂ /MnP6	99	~100	5.0

210 ^a mean and standard deviation.

211

212 In situ derivatization and covalent immobilization yield of MnPs onto Sil-Cl
 213 were on average greater than 90%, whereas electrostatic immobilization of MnPY
 214 onto SiO₂ was essentially quantitative (Table 1), which is in direct contrast with
 215 the related SBA-15 and HMS systems where immobilization yields were ~60%
 216 and ~28% on average, respectively, for similar MnP loadings.¹⁻³ The

217 immobilization yields of ca. 100% for the three cationic MnPY (Y = 4, 5, 6) isomers
218 indicates that higher loads of MnP on SiO₂ may be achieved, but this was not
219 investigated herein; materials of high metalloporphyrin loads have not resulted in
220 better oxidation catalysts in previous studies.¹³

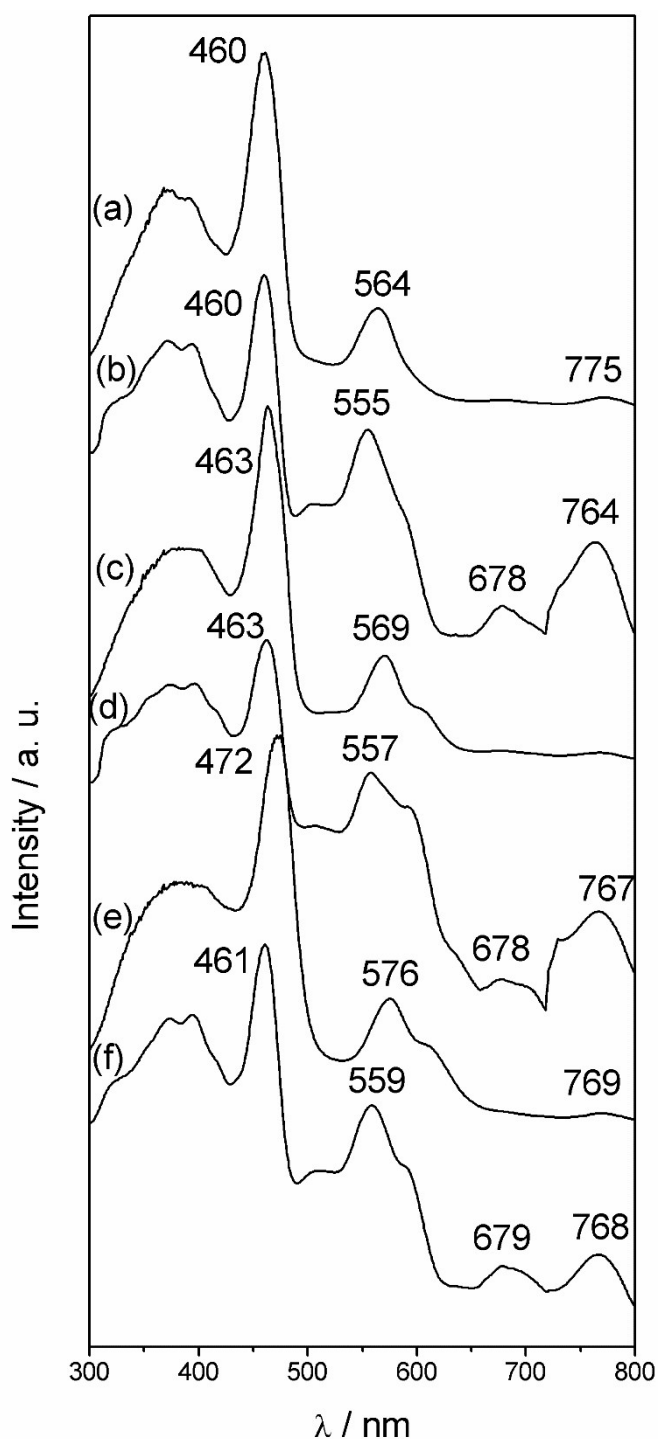
221 Immobilization of neutral **(1)**, **(2)**, **(3)** onto non-modified silica gel (SiO₂),
222 which lacks the possibility for in situ covalent derivatization of these Mn
223 porphyrins, yielded MnP-containing materials of little interest, as weakly
224 adsorbed **(1)**, **(2)**, or **(3)** were essentially fully leached with a variety of organic
225 solvents (MeOH, EtOH, MeCN, and mixtures with CH₂Cl₂ or CHCl₃); this is
226 consistent with the reported behavior of these neutral MnPs toward regular
227 chromatographic SiO₂ and related data on mesoporous SBA-15 silica.^{1,4}
228 Conversely, all attempts to release MnP from **SiI-CI/MnPY** (Y = 1, 2, 3) and
229 **SiO₂/MnPY** (Y = 4, 5, 6) materials *via* extraction with either water or organic
230 solvents (MeOH, MeCN, EtOH, CHCl₃) were unsuccessful, revealing the stability
231 of these materials against MnP leaching. Release of MnP from these materials
232 was achieved only under drastic conditions *via* silica matrix dissolution with
233 concentrated aqueous NaOH. The present study was focused, thus, on the
234 **SiI-CI/MnPY** (Y = 1, 2, 3) and **SiO₂/MnPY** (Y = 4, 5, 6) materials.

235 The presence of MnPs on **SiI-CI/MnPY** (Y = 1, 2, 3) and **SiO₂/MnPY** (Y =
236 4, 5, 6) was confirmed by diffuse reflectance UV/VIS (DR-UV/VIS) of the
237 materials, given the high molar absorptivity of MnPs (see ESI, Section S4 and
238 S5) and their characteristic spectral features.⁹ Other routine characterization
239 techniques as elemental analysis, infrared spectroscopy, and thermoanalysis
240 were not able to detect the anchored MnPs due to their low loadings of about
241 0.3% (w/w). These limitations are consistent with previous heterogenized MnP
242 studies.^{2,13,21}

243 The DR-UV/VIS spectra of the three **SiI-CI/MnPY** (Y = 1, 2, 3) solids share
244 similar spectral profiles with the corresponding non-immobilized **(1)**, **(2)**, **(3)**
245 isomers (Fig. 2), which indicates that the structure of the porphyrin ring was
246 preserved during immobilization. Indeed, alkylation reactions of the peripheral
247 pyridyl moieties of Mn(III) *N*-pyridylporphyrins are accompanied by little spectral
248 profile changes (see ESI, Section S4). This behavior was also observed in our
249 previous work with mesoporous SBA-15 silica as support.¹ Only **SiI-CI/MnP3**,
250 which incorporates the *para* isomer, showed a redshift of the Soret band (Fig.

251 2e), possibly due to a perturbation of the π -electrons of the porphyrin macrocycle
252 provoked by the easier interaction with the support.^{21,47,48}

253

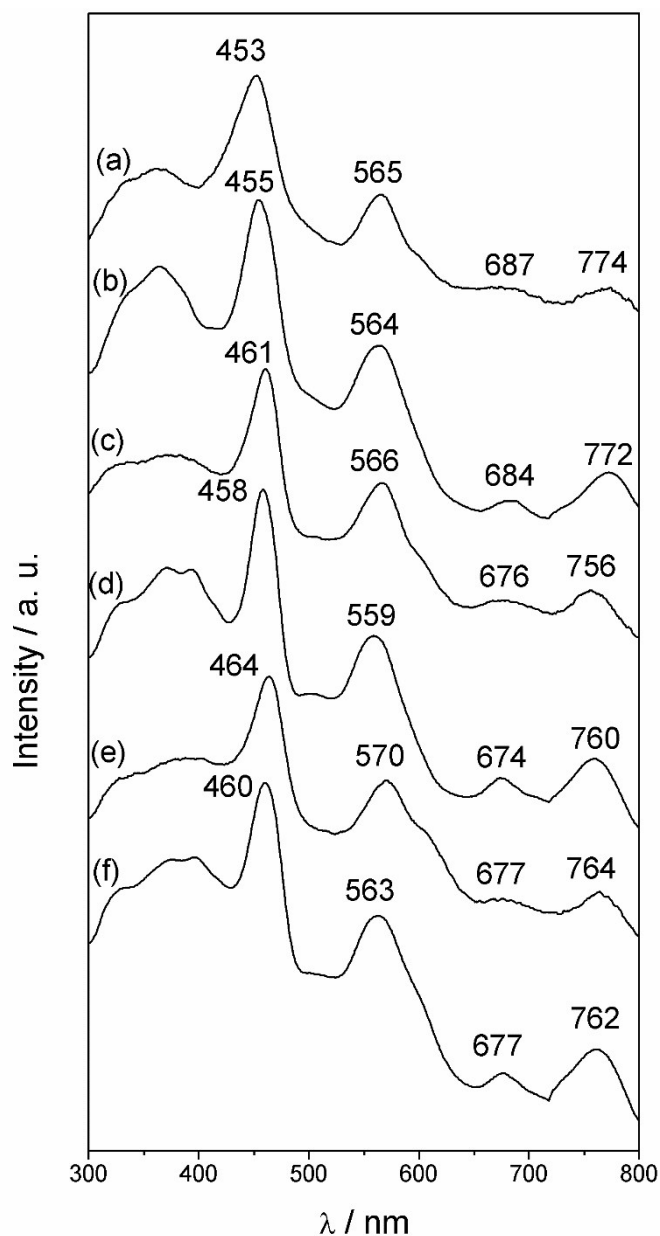


254

255 **Figure 2.** DR-UV/VIS spectra of the (a) **Sil-CI/MnP1**, (b) **(1)**, (c) **Sil-CI/MnP2**, (d)
256 **(2)**, (e) **Sil-CI/MnP3**, and (f) **(3)**. The spectra of non-immobilized MnPs were
257 recorded as solids dispersed on barium sulfate.

258

259 The DR-UV/VIS spectra of the three **SiO₂/MnPY** (**Y = 4, 5, 6**) solids are
 260 showed in Fig. 3. Again, the Soret band and the Q bands on these spectra were
 261 similar to those of the corresponding non-supported **MnPY**, indicating that the
 262 overall electronic structure of these systems is little affected by the electrostatic
 263 immobilization. This is consistent with previous observations on mesoporous
 264 SBA-15 and HMS systems.¹⁻³
 265

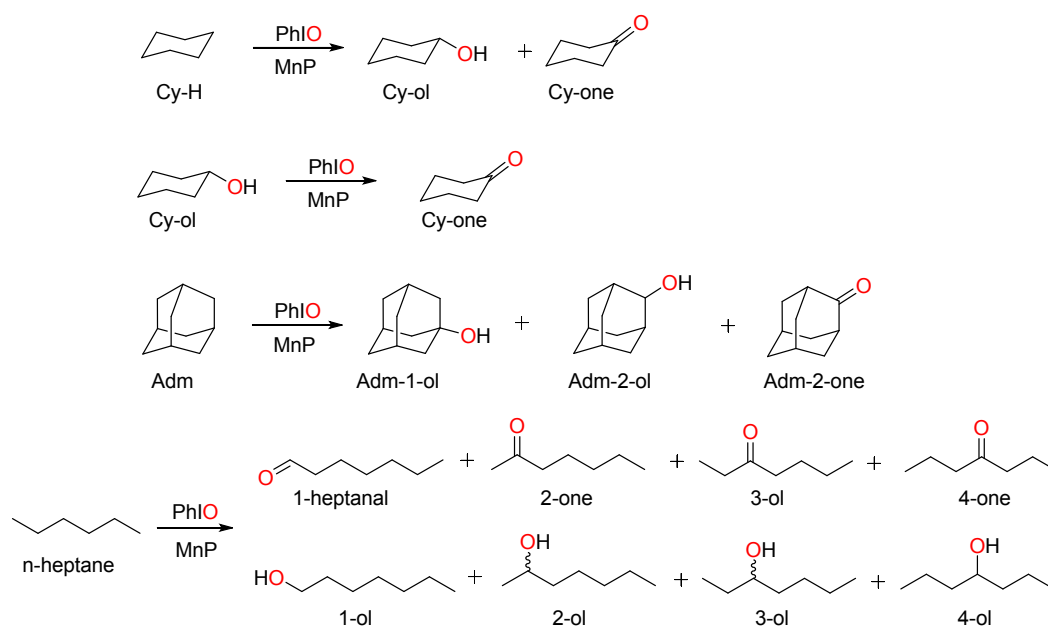


266
 267 **Figure 3.** DR-UV/VIS spectra of (a) **SiO₂/MnP4**, (b) **MnP4**, (c) **SiO₂/MnP5**, (d)
 268 **MnP5**, (e) **SiO₂/MnP6**, and (f) **MnP6**. The spectra of non-immobilized MnPs were
 269 recorded as solids dispersed on barium sulfate.

270

271 **Catalytic biomimetic oxidations**

272 The oxyfunctionalization of alkanes by C-H bond activation and/or
 273 selective oxidation under mild conditions remains a challenge in academia and
 274 industry and a much sought-after subject in catalysis.^{28-30,49-52} The efficiency of
 275 **SiI-Cl/MnP_Y** (**Y = 1, 2, 3**) and **SiO₂/MnP_Y** (**Y = 4, 5, 6**) materials as catalysts for
 276 C-H activation *via* alkane hydroxylation was evaluated in typical
 277 metalloporphyrin-based model reactions using cyclohexane, n-heptane, and
 278 adamantane as substrates and iodosylbenzene (PhIO) as oxidant (Fig. 4).
 279 Oxidation of cyclohexanol was also carried out to uncover some features of
 280 ketone formation in these systems. In all cases, reactions with the corresponding
 281 non-immobilized MnPs ((**1**), (**2**), (**3**) or **MnP_Y**) under homogeneous conditions
 282 were carried out to evaluate the role played by the support on catalytic efficiency
 283 and reaction selectivity. Chloride salts of the cationic **MnP_Y** (**X = 4, 5, 6**) isomers
 284 are, however, poorly soluble in 1:1 (v/v) MeCN:CHCl₃ solvent mixture used in the
 285 oxidation reactions. Thus, the corresponding tosylate salts of **MnP_Y**, which are
 286 soluble in MeCN:CHCl₃ solvent mixtures, were used in the homogeneous
 287 reactions. Herein, the product yields for alkane oxidations were calculated based
 288 on the initial amount of PhIO (limiting reactant), considering a 1:1 stoichiometry
 289 for alcohols and 2:1 stoichiometry for aldehyde and ketones.^{1,4,12}



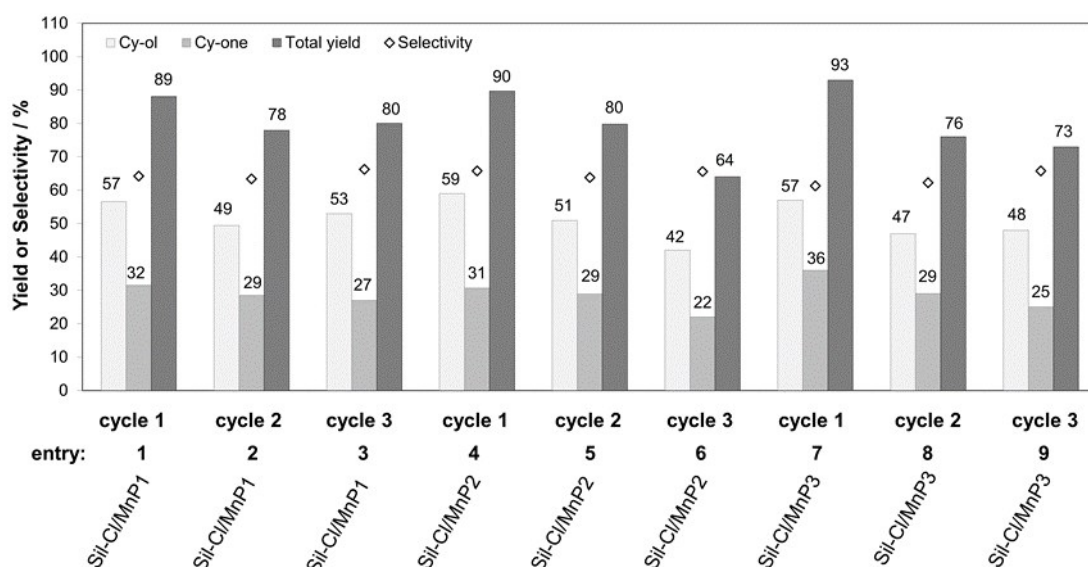
290

291 **Figure 4.** Reaction schemes for the oxidation of cyclohexane (Cy-H),
 292 cyclohexanol (Cy-ol), n-heptane, and adamantane (Adm) catalyzed by
 293 homogeneous and immobilized MnPs studied in this work.

294

295 **Cyclohexane as model substrate**

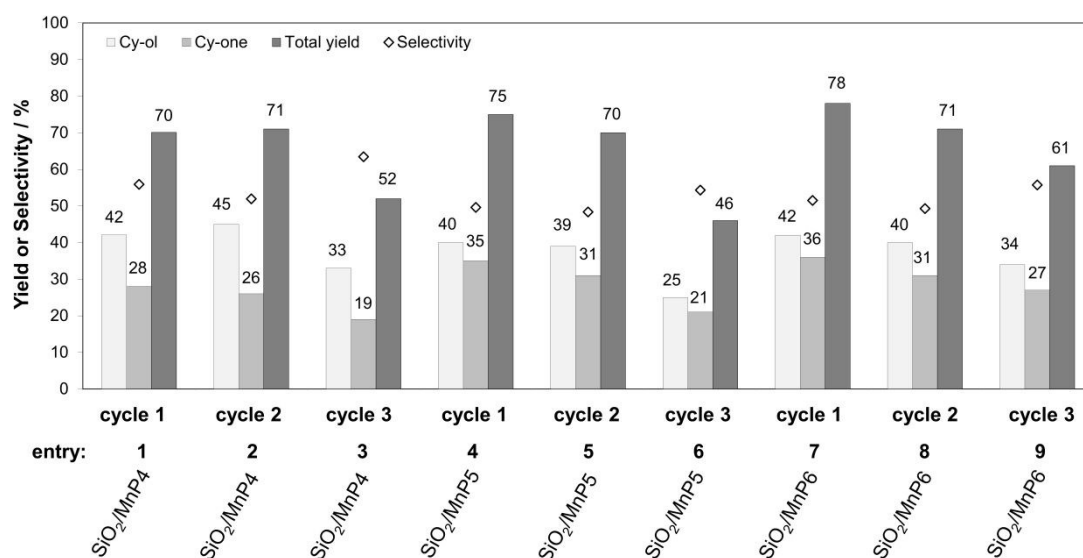
296 Cyclohexanol (Cy-ol) and cyclohexanone (Cy-one) yields and Cy-ol selectivity for
 297 cyclohexane (Cy-H) oxidation catalyzed by the heterogenized materials **Sil-**
 298 **Cl/MnP_Y** (**Y = 1, 2, 3**) and **SiO₂/MnP_Y** (**Y = 4, 5, 6**) for three independent catalytic
 299 cycles are presented in Figures 5 and 6, respectively. The data for all control
 300 reactions, including the homogeneous systems with the non-immobilized Mn
 301 porphyrins, are given in ESI (Section 10, Fig. S15). All reactions were carried out
 302 using a MnP/PhIO/Cy-H molar ratio of 1:10:4628. In the control reactions of Cy-
 303 H with PhIO alone, **SiO₂/PhIO**, or **Sil-Cl/PhIO**, a low total yield (Cy-ol + Cy-one)
 304 of about 2% was observed, indicating that the supports SiO₂ or Sil-Cl were unable
 305 to catalyze efficiently the PhIO-oxidation of cyclohexane in the absence of Mn
 306 porphyrin (ESI, Section 10, Fig. S15).



307

308 **Figure 5.** First (cycle 1), second (cycle 2), and third (cycle 3) cycles of
 309 cyclohexane oxidation reactions by PhIO catalyzed by the supported materials
 310 **Sil-Cl/MnP_Y** (**Y = 1, 2, 3**). After completion of each cycle, the catalysts were
 311 recovery and reused. Reactions conditions: MnP/PhIO/Cy-H molar ratio of
 312 1:10:4628 (0.2 μmol of MnP, 2.0 μmol of PhIO, 930.0 μmol of Cy-H),
 313 MeCN:CHCl₃ mixture (1:1, v/v) as solvent, magnetic stirring, 26 °C, 90 min, and
 314 air atmosphere. Yields calculated based on the starting PhIO. 2 mol of PhIO were
 315 considered for the formation of 1 mol of Cy-one. Total yield = Cy-ol + Cy-one.
 316 Selectivity = 100 x [Cy-ol/(Cy-ol + Cy-one)].

317

View Article Online
DOI: 10.1039/D0DT01383H

318

319 **Figure 6.** First (cycle 1), second (cycle 2), and third (cycle 3) cycles of
 320 cyclohexane oxidation reactions by PhIO catalyzed by the supported materials
 321 **SiO₂/MnP_Y** (**Y = 4, 5, 6**). After completion of each cycle, the catalysts were
 322 recovery and reused. The reaction conditions were identical to those of Figure 5.
 323 Yields calculated based on the starting PhIO. 2 mol of PhIO were considered for
 324 the formation of 1 mol of Cy-one. Total yield = Cy-ol + Cy-one. Selectivity = 100
 325 x [Cy-ol/(Cy-ol + Cy-one)].

326

327

328

329

330

331

332

333

334

335

336

337

338

A comparison between the supported MnPs systems (on either **SiI-CI** or **SiO₂**) (Figs. 5 and 6) with their corresponding non-immobilized MnP counterparts (ESI, Fig. S15) reveals a considerable increase in the total oxidation yield (Cy-ol + Cy-one) for all heterogenized systems **SiI-CI/MnP_Y** or **SiO₂/MnP_Y**. A likely explanation, which is supported by recycling experiments (see below) is related to the increased oxidative stability of MnPs upon immobilization on either **SiI-CI/MnP_Y** (**Y = 1, 2, 3**) or **SiO₂/MnP_Y** (**Y = 4, 5, 6**) materials as compared with their corresponding homogeneous systems. Of note, **(1), (2), (3)** and **MnP_Y** (**Y = 4, 5, 6**) in homogeneous systems showed oxidative destruction (bleaching) of about 70%, as determined spectrophotometrically in the end of the reactions. The role of inert supports in the increased oxidative stability of MnPs is well documented.^{12,26,53,54}

339 The highest Cy-ol selectivities were observed in the **Sil-CI/MnPY (Y = 1, 2, 3)** solids and this may also be related to a role played by the nature of the
340 support. **Sil-CI/MnPY** solids (Fig. 5, entries 1, 4, and 7) showed an overall 10%
341 higher selectivity and 20% higher total yield than **SiO₂/MnPY** solids (Fig. 6,
342 entries 1, 4, and 7). As suggested in the SBA-15 related systems,¹ this may
343 tentatively be related to the lipophilic character of **Sil-CI** (given the excess surface
344 chloropropyl moieties) as compared to the more polar nature of unmodified **SiO₂**.
345 This may facilitate the access of apolar Cy-H substrate) and the replacement of
346 polar Cy-ol product from the catalytic center, resembling the protein role in
347 cytochromes P450.¹¹ Proper experiments need, however, to be designed and
348 carried out to unambiguously assess this surface lipophilic effects on catalysis.
349

350 **Sil-CI/MnPY (Y = 1, 2, 3)** catalysts based on cheap, ordinary,
351 chromatographic silica were more efficient and equally selective for cyclohexane
352 oxidation than the more elaborate SBA-15Cl-based catalyst counterparts.¹ The
353 total oxidation yields achieved with **Sil-CI/MnP1**, **Sil-CI/MnP2**, and **Sil-CI/MnP3**
354 were of 89, 91, and 93%, respectively (Fig. 5, entries 1, 4, and 7), which contrasts
355 with those of 54, 62, and 72% reported for SBA-15Cl-based catalysts SBA-
356 15Cl/MnP1, SBA-15Cl/MnP2, and SBA-15Cl/MnP3, respectively.¹ This
357 difference in overall efficiency between **Sil-CI/MnPY (Y = 1, 2, 3)** and
358 SBA-15Cl/MnPY (Y = 1, 2, 3) may be related to the localization of the MnPs on
359 the supports. Lower yields with mesoporous SBA-15Cl/MnPY (Y = 1, 2, 3)
360 materials have suggested that MnP is probably buried inside the mesoporous,
361 hindering access of substrate and oxidant.¹ Conversely, for **Sil-CI/MnPY**
362 catalysts, we speculate that MnPs are predominantly exposed on the material
363 surface, favoring the catalytic reaction.⁵⁵⁻⁵⁷ A similar behavior was observed with
364 the **SiO₂/MnPY** catalysts when compared to their analogous SBA-15/MnPY
365 materials: total yields achieved with **SiO₂/MnPY** solids (aprox. 74%, Fig. 6,
366 entries 1, 4, and 7) were remarkably higher than those with SBA-15/MnPY
367 materials (aprox. 45%).¹

368 **Sil-CI/MnPY (Y = 1, 2, 3)** and **SiO₂/MnPY (Y = 4, 5, 6)** were evaluated in
369 recycling reactions (Fig. 5 and 6). All immobilized catalysts maintained a high
370 overall yield, particularly in cycle 2, with some loss in efficiency on cycle 3. The
371 Cy-ol selectivity of the reactions were essentially unaffected, at least during 3

372 cycles. These results are in direct contrast to those of SBA-15 systems, where
373 overall yields were reduced by approx. 50% in the second cycle already.¹

374 **Sil-Cl/MnP1** material was the most robust catalyst among all supported
375 MnPs, showing an efficiency loss of only 10% (Fig. 5, entries 1-3) during the three
376 oxidation reaction cycles. **SiO₂/MnP4** and **SiO₂/MnP6** catalysts had an efficiency
377 loss of 18% and 16%, respectively (Fig. 6, entries 4-6 and 7-9). Conversely,
378 **SiO₂/MnP5** catalyst showed the largest loss (ca. 29%) in efficiency by the end of
379 the third reaction cycle (Fig. 6, entries 1-3). The decrease in catalytic efficiency
380 throughout the recycling reactions was ascribed to oxidative destruction of
381 supported MnP (bleaching) along the oxidation cycles, as in other related
382 systems.^{58,59} MnP leaching was considered of lower impact (if any) as no sign of
383 MnP in the reaction supernatant or catalyst washing solvents has been detected
384 by UV/VIS spectroscopy.

385 The oxidative stability of the heterogenized catalysts (**Sil-Cl/MnP_Y** and
386 **SiO₂/MnP_Y**) was evaluated using a more drastic condition with a PhIO/MnP
387 molar ratio of 100 in the first reaction cycle (cycle A) followed by the standard
388 reaction condition with a PhIO/MnP molar ratio of 10 in the second reaction cycle
389 (cycle B), as similarly carried out in the literature SBA-15-based systems.¹ The
390 non-immobilized catalysts were also studied under homogeneous conditions with
391 PhIO/MnP molar ratio of 100 (cycle A) for comparison with the corresponding
392 heterogenized systems. All data for these reactions are presented in ESI (Section
393 11, Figs. S16 and S17). The PhIO, **Sil-Cl/PhIO**, and **SiO₂/PhIO** control systems
394 (without MnP) showed less than 1% Cy-ol and Cy-one formation.

395 All catalysts showed low catalytic efficiency with a high PhIO/MnP molar
396 ratio of 100 (Cycle A; ESI Fig. S16). Upon catalyst reuse under standard
397 PhIO/MnP ratio of 10 (Cycle B; ESI Fig. S17), all catalysts recovered, at least
398 partially, the efficiency recorded in Figs. 5 and 6. A more general discussion and
399 some hypotheses^{1,21,54,60-63} on these results are presented in ESI (Section 11).
400 Briefly, they indicate that (a) the materials are to some extent reasonably stable
401 against oxidative degradation under large excess PhIO; (b) SiO₂-based materials
402 were more resist than the corresponding Sil-Cl ones, in agreement with previous
403 data on the SBA-15-based catalysts;¹ (c) the remarkable stability of **Sil-Cl/MnP1**
404 and **SiO₂/MnP4** may be associated with the recurring porphyrin-based
405 biomimetic feature known as “the *ortho* effect”,^{4,38,54,64-66} in which the *ortho*,

406 surface-derived 2-*N*-propylpyridinium groups on **Sil-Cl/MnP1** (Fig. 1) and the
407 *ortho* 2-*N*-methylpyridinium groups on **SiO₂/MnP4** (Fig. 1) may hamper oxidative
408 attack to vulnerable porphyrin *meso* positions.

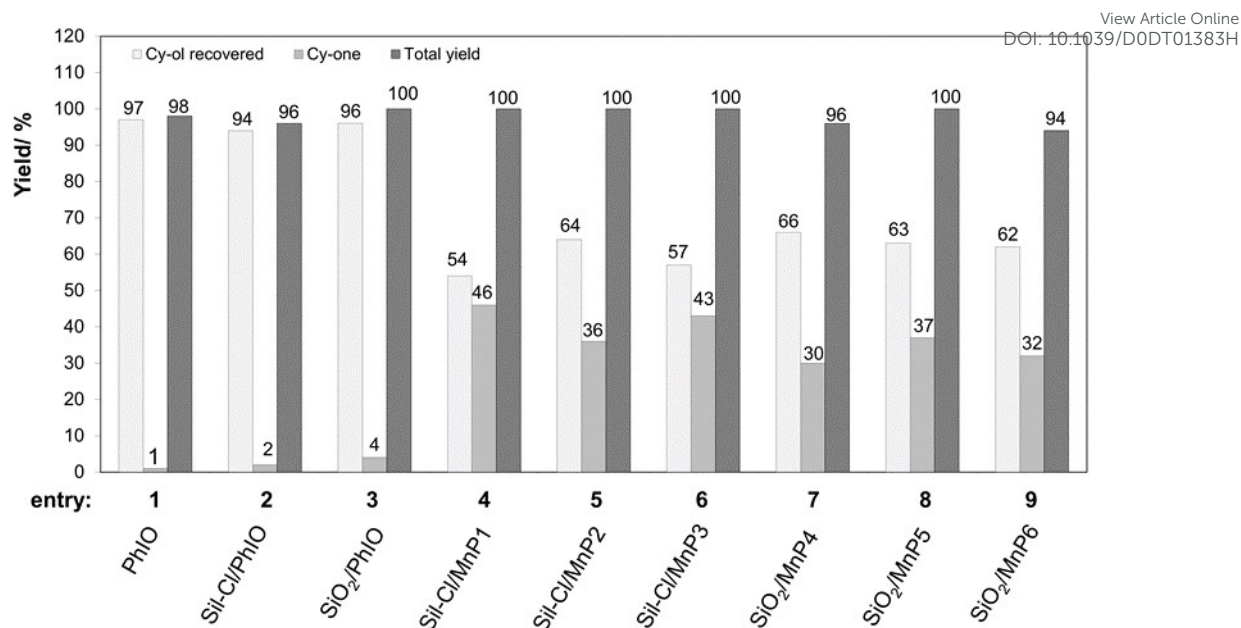
409

410 **Cyclohexanol as model substrate**

411 **Si-Cl/MnP_Y** (**Y = 1, 2, 3**) and **SiO₂/MnP_Y** (**Y = 4, 5, 6**) were evaluated as
412 catalysts in the oxidation of Cy-ol to Cy-one by PhIO as a means to verify whether
413 Cy-one produced during the cyclohexane oxidation could result from Cy-ol
414 product being further oxidized. In these studies using Cy-ol as substrate, the
415 amount of initial Cy-ol was established considering the maximum theoretical
416 concentration of Cy-ol corresponding to a 100% yield in the cyclohexane
417 oxidations, that is, a stoichiometric molar Cy-ol/MnP of 10:1. Cy-one yields were
418 based on the initial PhIO (limiting reactant), considering 1 mol of PhIO for the
419 formation of 1 mol of Cy-one.

420 All materials were able to catalyze the Cy-ol oxidation to Cy-one to some
421 extent (Fig. 7), indicating, thus, that the ketone formed in the cyclohexane
422 oxidation may be derived from Cy-ol product reoxidation. Metalloporphyrin-
423 catalyzed oxidation of alcohol to ketones has been addressed.⁶⁷⁻⁶⁹ However, the
424 formation of ketone in alkane oxidations *via* alternative mechanisms, involving
425 radical reactions^{55,70,71} cannot be completely ruled out.⁷² Regardless of the
426 mechanism(s), in the Cy-ol oxidations catalyzed by **Sil-Cl/MnP_Y** (**Y = 1, 2, 3**) and
427 **SiO₂/MnP_Y** (**Y = 4, 5, 6**), the Cy-one yields were relatively high and comparable
428 to those of the cyclohexane oxidation (Fig. 5). Among these systems, **Sil-**
429 **Cl/MnP1** and **Sil-Cl/MnP3** showed slightly better catalytic performances than the
430 others (Fig. 7, entry 4 and 6).

431

View Article Online
DOI: 10.1039/D0DT01383H

432

433 **Figure 7.** Cyclohexanol oxidation by PhIO catalyzed by supported materials
 434 **Sil-Cl/MnP** (Y = 1, 2, 3) and **SiO₂/MnP** (Y = 4, 5, 6), including the control
 435 reactions (PhIO, **Sil-Cl/PhIO**, and **SiO₂/PhIO**). The reaction conditions were
 436 identical to those of Figure 5 except that Cy-ol replaced cyclohexane and the
 437 MnP/PhIO/Cy-ol molar ratio was of 1:10:10. Yields calculated based on the
 438 starting PhIO. 1 mol of PhIO was considered for the formation of 1 mol of Cy-one.
 439 Total yield = Cy-ol + Cy-one.

440

441 These preliminary results on Cy-ol oxidation indicate that the
 442 heterogenized MnP materials **Sil-Cl/MnP** (Y = 1, 2, 3) and **SiO₂/MnP** (Y = 4,
 443 **5, 6**) are potentially effective catalysts for alcohol oxidation and deserve, thus,
 444 further investigation.^{73,74}

445

446 **n-Heptane as model substrate**

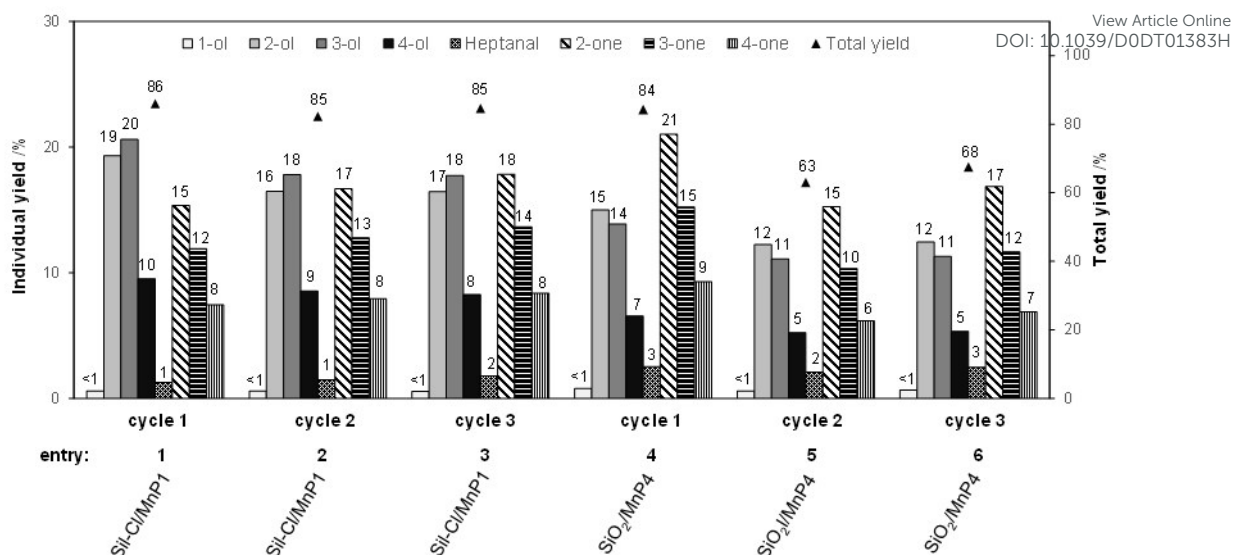
447 n-Heptane is a fairly stable acyclic alkane difficult to be oxyfunctionalized
 448 due to the inertness of its C–H bonds, whose energies are higher for the primary
 449 carbons ($101 \pm 1.8 \text{ kcal mol}^{-1}$) than for the secondary ones ($98 \pm 1.8 \text{ kcal mol}^{-1}$).⁷⁵
 450 The selective oxidation of linear alkanes at the primary carbons is highly sought
 451 and remains a challenge.

452 The heterogenized catalysts **Sil-Cl/MnP** (Y = 1, 2, 3) and **SiO₂/MnP** (Y
 453 = 4, 5, 6) were evaluated for the PhIO-oxidation reactions of n-heptane using a

454 MnP/PhIO/n-heptane molar ratio of 1:10:5000. The formation of eight oxidation
455 products (Fig. 4) were detected and independently quantified in all reactions: 1-
456 heptanol (1-ol), 2-heptanol (2-ol), 3-heptanol (3-ol), 4-heptanol (4-ol), 1-heptanal,
457 2-heptanone (2-one), 3-heptanone (3-one), and 4-heptanone (4-one). No
458 attempts were undertaken to resolve the stereochemistry of 2-ol and 3-ol. This
459 range of oxidation product has been partially reported with related immobilized
460 metalloporphyrin-based catalytic systems.^{2,76-78} The n-heptane oxidations were
461 evaluated for **SiI-CI/MnPY** (**Y = 1, 2, 3**) and **SiO₂/MnPY** (**Y = 4, 5, 6**) catalytic
462 efficiency, reaction chemo- and regioselectivity, and catalyst recycling. The
463 product yields for three oxidation cycles with **SiI-CI/MnP1** and **SiO₂/MnP4**, as
464 representatives of each catalyst class, is presented in Figure 8. Data for the other
465 materials along with the homogeneous systems are in ESI (Section 12, Figs. S18
466 – S20).

467 In the first cycle of n-heptane oxidation reactions, the control systems
468 (PhIO, **SiO₂/PhIO**, and **SiI-CI/PhIO**) led to total product yield lower than 5% (data
469 not shown). Conversely, total oxidation yields in the 66 – 95% range with the
470 supported catalysts **SiI-CI/MnPY** (**Y = 1, 2, 3**) and **SiO₂/MnPY** (**Y = 4, 5, 6**) under
471 heterogeneous conditions (Fig. 8 and ESI Figs. S18 and S19) were unusually
472 high for n-heptane oxidation catalyzed by metalloporphyrin-based materials.^{5,25}
473 The high catalytic efficiency of these material is also in direct contrast with the 33
474 – 68% total yield range found with the non-immobilized catalysts under
475 homogeneous conditions (ESI, Fig. S20). This substantial increase in total
476 oxidation yield with the heterogenized catalysts **SiI-CI/MnPY** (**Y = 1, 2, 3**) and
477 **SiO₂/MnPY** (**Y = 4, 5, 6**) is likely associated with the remarkable impact of the
478 support on stabilizing the anchored MnPs against oxidative degradation, as
479 observed in the cyclohexane systems. Of note, non-immobilized MnPs were
480 bleached by approx. 40% [for **(1)**, **(2)**, **(3)**] and 50% (for **MnP4**, **MnP5**, **MnP6**),
481 respectively, during n-heptane oxidation.

482



483

484 **Figure 8.** First cycle (cycle 1), second (cycle 2), and third (cycle 3) cycles of n-
 485 heptane oxidation reactions by PhIO catalyzed by the supported materials **Sil-**
 486 **CI/MnP1** and **SiO₂/MnP4**. After completion of each cycle, the catalysts were
 487 recovery and reused. Reactions conditions: MnP/PhIO/n-heptane molar ratio of
 488 1:10:5000 (0.2 μmol of MnP, 2.0 μmol of PhIO, 1000.0 μmol of n-heptane),
 489 MeCN:CHCl₃ mixture (1:1, v/v) as solvent, magnetic stirring, 26 °C, 90 min, and
 490 air atmosphere. Yields calculated based on the starting PhIO. 2 mol of PhIO were
 491 considered for the formation of 1 mol of ketone or aldehyde. Total yield = 1-ol +
 492 2-ol + 3-ol + 4-ol + 1-heptanal + 2-one + 3-one + 4-one.

493

494 The overall superior efficiency of **Sil-CI/MnPY** (Y = 1, 2, 3) catalysts over
 495 **SiO₂/MnPY** (Y = 4, 5, 6) observed in Cy-H oxidations (Figs. 5 and 6) was more
 496 pronounced on the n-heptane systems, except that **SiO₂/MnP4** was as highly
 497 efficient as the **Sil-CI/MnPY** (Y = 1, 2, 3) catalysts (Fig. 8 and ESI Figs. S18 and
 498 S19). Another relevant feature of these materials revealed by the n-heptane
 499 oxidations relates to the remarkable change in chemoselectivity within these two
 500 classes of catalysts (Fig. 8 and Table 2). Whereas the **SiO₂/MnPY** (Y = 4, 5, 6)
 501 materials were more selective toward the carbonyl products (ketones and
 502 aldehyde), **Sil-CI/MnPY** (Y = 1, 2, 3) catalysts were more selective toward n-
 503 heptanols, corroborating once more the Cy-H data on the role played by the
 504 surface chloropropyl chain moieties of **Sil-CI** support in the oxidation reactions.
 505 Additionally, it is worth noting that non-immobilized (1), (2), and (3) shows
 506 chemoselectivity toward carbonyl products (Table 2 and ESI Fig. S20), indicating

507 that a full inversion in n-heptane oxidation chemoselectivity is observed upon
 508 MnP immobilization on the **SiI-CI** support to yield **SiI-CI/MnP_Y** (**Y = 1, 2, 3**)
 509 catalysts. As described for the Cy-H oxidation reactions, it is suggested that the
 510 chloropropyl chains on **SiI-CI** renders **SiI-CI/MnP_Y** (**Y = 1, 2, 3**) catalysts likely
 511 more lipophilic, facilitating the approach of n-heptane to the materials surface and
 512 the access to the MnP catalytic sites, thus resulting in a high chemoselectivity for
 513 alcohol. The possible role of surface chloropropyl chains in repealing n-heptanols
 514 from the catalyst active sites, preventing, thus, further oxidation to carbonyl
 515 products cannot be fully assessed or ruled out at the moment without further
 516 investigation.

517
 518 **Table 2.** Chemoselectivity and Regioselectivity of n-heptane PhIO-oxidations
 519 catalyzed by **SiI-CI/MnP_Y** (**Y = 1, 2, 3**) and **SiO₂/MnP_Y** (**Y = 4, 5, 6**) under
 520 heterogeneous conditions or by non-immobilized MnPs under homogeneous
 521 conditions. The reaction conditions are indicated in Figure 8.

Entry	Catalyst	Total yield /%		Chemoselect. ^c /%	Regioselectivity ^g /%		
		C-OH ^a	C=O ^b		ω -1 ^d	ω -2 ^e	ω -3 ^f
1	SiI-CI/MnP1	50	36	58	34	32	33
2	SiI-CI/MnP2	51	40	56	33	32	34
3	SiI-CI/MnP3	51	44	54	32	32	35
4	SiO₂/MnP4	36	48	43	36	30	32
5	SiO₂/MnP5	24	42	36	34	30	34
6	SiO₂/MnP6	24	42	36	34	28	36
7	(1)	16	46	26	26	32	41
8	(2)	23	44	35	21	32	46
9	(3)	19	42	31	22	32	44
10	MnP4	11	15	43	35	28	33
11	MnP5	11	20	35	22	31	43
12	MnP6	15	18	45	32	32	35

522 ^a C-OH (alcohols) = 1-ol + 2-ol + 3-ol + 4-ol. ^b C=O (ketones + aldehyde) = 1-heptanal +
 523 2-one + 3-one + 4-one. ^c Chemoselectivity = (C-OH)/(C-OH + C=O). ^d ω -1: sum of 2-ol
 524 and 2-one, ^e ω -2: sum of 3-ol and 3-one, ^f ω -3: sum of 4-ol and 4-one. ^g Normalized
 525 regioselectivity (ω -1) = 100 x [(2-ol + 2-one)/2]/{[(1-ol+1-heptanal)/3] + [(2-ol + 2-one)/2]}

526 + [(3-ol + 3-one)/2] + (4-ol + 4-one)}, normalized regioselectivity (ω -2) and normalized
527 regioselectivity (ω -3) were calculated analogously.

528

529 n-Heptane is a substrate that allows also for the evaluation of
530 regioselectivity associated with the catalyzed oxidations. Considering that n-
531 heptane primary carbons ω (C1 and C7 positions) have a total of 6 C-H bonds,
532 the secondary carbons ω -1 (C2 and C6 positions) and ω -2 (C3 and C5 positions)
533 have a total of 8 C-H bonds, and central secondary carbon ω -3 (C4 position) has
534 only 2 C-H bonds, all regioselectivities associated with ω , ω -1, ω -2, and ω -3
535 carbons were normalized to account for the statistical probability of n-heptane
536 oxidation on each position (Table 2). The regioselectivity of oxidations catalyzed
537 by the heterogenized catalysts **Sil-CI/MnPY** (**Y = 1, 2, 3**) and **SiO₂/MnPY** (**Y = 4,**
538 **5, 6**) was under thermodynamic control, that is, oxyfunctionalization of the primary
539 carbons was very low (ω regioselectivity was lower than 2% in all cases) and ω -
540 1 (sum of 2-ol and 2-one), ω -2 (sum of 3-ol and 3-one), and ω -3 (sum of 4-ol and
541 4-one) regioselectivities were nearly the same, indicating that there was no
542 oxidation preference among the secondary carbons. Thus, the silica support or
543 surface organic chain of **Sil-CI** did not exert any significant influence (if any) in
544 guiding the orientation of n-heptane toward the catalytic center.

545 After the first oxidation cycle, the supported catalysts **Sil-CI/MnPY** (**Y = 1,**
546 **2, 3**) and **SiO₂/MnPY** (**Y = 4, 5, 6**) were centrifuged, washed with CHCl₃, EtOH,
547 MeOH, and H₂O, dried at 80 °C for 24 h, and reused (cycle 2) under the same
548 reaction condition as those of the first cycle (Fig. 8 and ESI Figs. S18 and S19).
549 This process was repeated once more, giving rise to a third cycle (cycle 3) (Fig.
550 8 and ESI Figs. S18 and S19). The robustness of **Sil-CI/MnP1** and **Sil-CI/MnP3**
551 as oxidation catalysts, as observed earlier in the cyclohexane systems, was also
552 confirmed in the n-heptane reactions; the total oxidation yields associated with
553 these catalysts were very high (in the 82 – 95% range) and just slightly affected
554 by reuse for at least three oxidation cycles. The corresponding *meta* MnP isomer-
555 based heterogenized catalysts **Sil-CI/MnP2** and **SiO₂/MnP5**, however, showed
556 considerable loss of efficiency upon recycling (ESI Fig. S18), as also observed in
557 the cyclohexane oxidations. In general, the **Sil-CI/MnPY** (**Y = 1, 2, 3**) catalysts
558 were more resistant against oxidative deactivation than the corresponding
559 **SiO₂/MnPY** (**Y = 4, 5, 6**) materials.

560 Despite the catalytic efficiency of **Sil-Cl/MnPY (Y = 1, 2, 3)** being little
561 affected by catalyst recycle in n-heptane oxidations, the chemoselectivity of these
562 reactions were compromised along the three reuses, particularly from the 1st to
563 the 2nd cycles (Table 2, entries 1–3; and ESI Tables S4 and S5, entries 1–3).
564 Such a selectivity decrease was not observed in cyclohexane oxidation catalyzed
565 by these **Sil-Cl/MnPY (Y = 1, 2, 3)** materials. Given the closer structural similarity
566 of the surface chloropropyl moieties to n-heptane rather than to cyclohexane, it
567 is tempting to suggest that some partial destruction of these surface chloropropyl
568 groups (as a somewhat competing substrate during n-heptane oxidation), may
569 be likely responsible to decrease the lipophilicity of Sil-Cl surface. This, hence,
570 would facilitate the access of n-heptanols to the MnP catalytic center, promoting
571 their further oxidation to the corresponding carbonyl derivatives and, finally,
572 compromising chemoselectivity for alcohols upon catalyst reuse. Whereas the
573 putative cumulative oxidation of surface chloropropyl moieties would decrease
574 chemoselectivity, it may also represent a sacrificial means to protect surface MnP
575 against oxidative destruction, which is, thus, consistent with little effect on **Sil-**
576 **Cl/MnPY (Y = 1, 2, 3)** catalyst efficiency upon recycling. Conversely, it is worth
577 noting that the chemoselectivity of the n-hexane oxidations catalyzed by
578 **SiO₂/MnPY (Y = 4, 5, 6)** remains essentially unchanged upon recycling; **SiO₂**
579 support, as opposed to **Sil-Cl**, is not prone to PhIO modification and the decrease
580 in catalyst efficiency observed with the **SiO₂/MnPY (Y = 4, 5, 6)** systems may be
581 a result of direct surface **MnPY** degradation during reuse; this is consistent with
582 a direct effect on efficiency, but of little impact on chemoselectivity.

583 Catalyst recycling exert little effect on regioselectivity of n-heptane
584 oxidation catalyzed by **Sil-Cl/MnPY (Y = 1, 2, 3)** and **SiO₂/MnPY (Y = 4, 5, 6)**
585 (Table 2 and ESI Tables S4, and S5).

586

587 **Adamantane as model substrate**

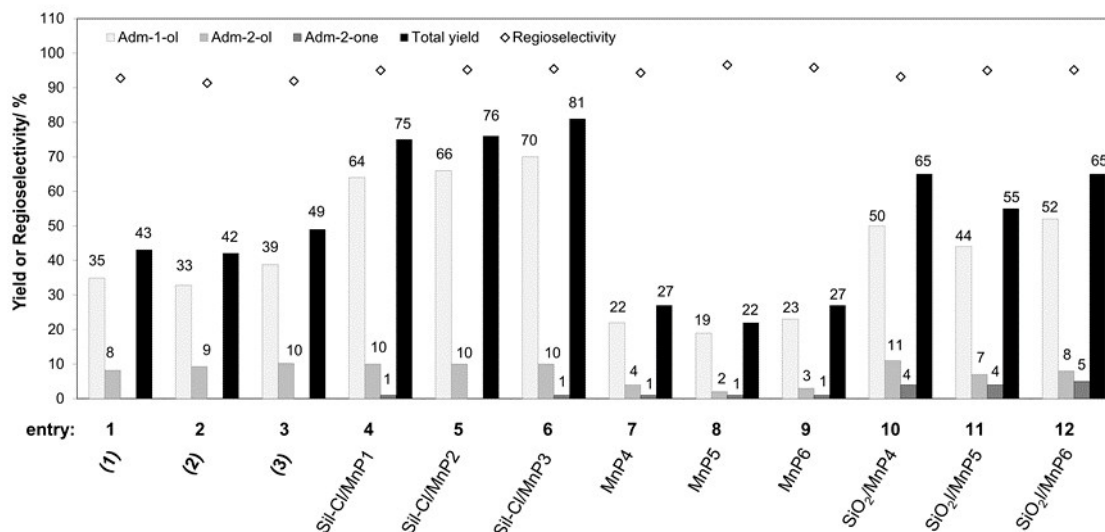
588 The adamantane is a substrate bulkier and conformationally more rigid
589 than cyclohexane and n-heptane. The oxidation in its tertiary carbons results in
590 1-adamantanol (Adm-1-ol), whereas oxidation in its secondary carbons results in
591 either 2-adamantanol (Adm-2-ol) or adamantanone (Adm-2-one), as depicted in
592 Figure 4.^{54,79-82}

593 Figure 9 summarizes the data obtained on adamantane oxidation
594 catalyzed by the heterogenized catalysts **SiI-CI/MnPY** (**Y = 1, 2, 3**) and
595 **SiO₂/MnPY** (**Y = 4, 5, 6**) and their homogeneous MnP counterparts. Control
596 experiments (PhIO, **SiI-CI/PhIO**, and **SiO₂/PhIO**) in absence of catalysts showed
597 total oxidation yields as little as 6%. Under homogeneous conditions, **(1)**, **(2)**, and
598 **(3)** isomers were equally efficient among themselves (45% on average; Fig. 9
599 entries 1-3) and more efficient than homogeneous **MnPY** (**Y = 4, 5, 6**) (25% on
600 average, Fig. 9, entries 7-9). A considerable increase in catalytic efficiency was
601 achieved upon heterogenization, as observed previously in the cyclohexane and
602 n-heptane systems; total oxidation yields for adamantane oxidations catalyzed by
603 **SiI-CI/MnPY** (**Y = 1, 2, 3**) and **SiO₂/MnPY** (**Y = 4, 5, 6**) ranged from 55% to 81%
604 (Fig. 9, entries 4-6, 10-12). Such an efficiency improvement may be attributed to
605 the role played by the support in increasing the oxidative stability of immobilized
606 MnPs. Total oxidation yields achieved with **SiI-CI/MnPY** (**Y = 1, 2, 3**) catalysts
607 (77% on average, Fig. 9, entries 4-6) were approx. 15% greater than those with
608 **SiO₂/MnPY** (**Y = 4, 5, 6**) catalysts (62% on average, Fig. 9, entries 10-12), which
609 may tentatively be related to the lipophilicity of **SiI-CI** surface as discussed for the
610 cyclohexane and n-heptane oxidations.

611 In all systems, hydroxylation was the main reaction observed giving rise to
612 Adm-1-ol and Adm-2-ol. Except in the **SiO₂/MnPY** (**Y = 4, 5, 6**) systems, in which
613 further Adm-2-ol oxidation led to Adm-2-one in yields as low as 5% (Fig. 9, entries
614 10-12), the formation of ketone in all other systems was lower than 1%, if any.
615 Whereas such small but measurable effect may perhaps be related to the
616 hydrophilic nature of SiO₂ support in **SiO₂/MnPY** (**Y = 4, 5, 6**) catalysts, analyses
617 of chemoselectivity were of little relevance in these adamantane-based model
618 reactions.

619 Regarding reaction regioselectivity, all catalysts studied herein were
620 selective toward hydroxylation of adamantane, chiefly at its tertiary carbon to yield
621 Adm-1-ol, following a similar behavior reported to other non-supported and
622 supported metalloporphyrin-based systems.^{54,79-81} The high preference toward
623 Adm-1-ol is ascribed to the lower C–H bond strength of adamantane tertiary
624 carbon, which results in its higher reactivity.^{79,82-84} In all systems, regioselectivity
625 was normalized with respect to the statistical probability of the oxidation associate

626 with the number of C–H bonds, i.e., 4 tertiary C–H bonds to yield Adm-1-ol, and
627 12 secondary C–H bonds to yield Adm-2-ol and Adm-2-one.



628

629

630 **Figure 9.** First cycle (cycle 1) of adamantane oxidation by PhIO catalyzed by the
631 non-immobilized MnPs and the supported materials **SiI-CI/MnP_Y** (**Y = 1, 2, 3**)
632 and **SiO₂/MnP_Y** (**Y = 4, 5, 6**). Reactions conditions: MnP/PhIO/Adm molar ratio
633 of 1:10:500 (0.2 μmol of MnP, 2.0 μmol of PhIO, 100.0 μmol of Adm),
634 MeCN:CHCl₃ mixture (1:1, v/v) as solvent, magnetic stirring, 26 °C, 90 min, and
635 air atmosphere. Total yield = Adm-1-ol + Adm-2-ol + Adm-2-one. Yields
636 calculated based on the starting PhIO. 2 mol of PhIO were considered for the
637 formation of 1 mol of Adm-2-one. Normalized regioselectivity = 100 x (Adm-1-
638 ol)/[(Adm-1-ol) + (Adm-2-ol)/3 + (Adm-2-one)/3].

639

640 The total yield and regioselectivity of **SiI-CI/MnP_Y** (**Y = 1, 2, 3**) and
641 **SiO₂/MnP_Y** (**Y = 4, 5, 6**) catalysts were not changed over the three reaction
642 cycles (Fig. 9 and ESI, Section 13, Figs. S21 and S22).

643 Reuse of the supported catalysts **SiI-CI/MnP_Y** (**Y = 1, 2, 3**) and
644 **SiO₂/MnP_Y** (**Y = 4, 5, 6**) for two more cycles (cycles 2 and 3, ESI Figs. S21 and
645 S22) revealed that the reaction yields were little affected by catalyst recycling,
646 corroborating the results with the other model substrates that these materials are
647 particularly catalytically robust and resistant against oxidative degradation. The
648 small changes observed in product distribution upon catalyst recycling were
649 essentially limited to the **SiI-CI/MnP_Y** (**Y = 1, 2, 3**) systems, in which Adm-2-one

650 yields increased from less than 1% in the first cycle to ca 4% in the third cycle,
651 this was, however, of little impact on chemoselectivity as 1- and 2- adamantanol
652 account for more than 95% of total oxidation yields. Finally, it is worth noting that
653 the high efficiency and robustness observed for the **SiI-CI/MnP1** and
654 **SiI-CI/MnP4** catalysts in cyclohexane and n-heptane oxidations were also
655 observed in the adamantane oxidation reactions.

656

657

658 Conclusions

659 Chloropropyl-functionalized silica (**SiI-CI**) was used as support for direct
660 derivatization and covalent immobilization (quaternization reaction) of the three
661 Mn(III) *N*-pyridylporphyrin isomers in aqueous medium to yield **SiI-CI/MnPX** (**X=**
662 **1, 2, 3**). Additionally, **SiO₂/MnPY** (**Y= 4, 5, 6**) solids were prepared by the
663 electrostatic immobilization of the three cationic Mn(III) *N*-
664 methylpyridiniumporphyrin isomers on non-modified **SiO₂**.

665 The materials were evaluated as PhIO-oxidation catalysts for alkane
666 functionalization using cyclohexane, n-heptane, and adamantane as model
667 substrates. The strong bonding of MnPs with the inorganic matrices (**SiI-CI** and
668 **SiO₂**) resulted in heterogenized materials highly stable against leaching.

669 The supported materials **SiI-CI/MnPY** (**Y = 1, 2, 3**) and **SiO₂/MnPY** (**Y = 4,**
670 **5, 6**) showed good to excellent catalytic efficiency in all model substrate
671 oxidations. **SiI-CI/MnPY** (**Y = 1, 2, 3**) catalysts based on cheap, ordinary,
672 chromatographic silica were more efficient and equally selective for cyclohexane
673 oxidation than related literature SBA-15-based catalysts. The **SiI-CI/MnPY** (**Y =**
674 **1, 2, 3**) and **SiO₂/MnPY** (**Y = 4, 5, 6**) systems were also able to catalyze
675 cyclohexanol oxidation indicating that they are promising catalysts for alcohol
676 oxidation.

677 The supports played important roles in the catalytic efficiency, chemo- and
678 regioselectivity, and oxidative stability of heterogenized MnPs on the **SiI-**
679 **CI/MnPY** (**Y = 1, 2, 3**) and **SiO₂/MnPY** (**Y = 4, 5, 6**) materials. Although regular
680 chromatographic silicas are not expected to yield regioselectively noteworthy
681 catalysts, the study on the oxidation of n-heptane was particularly revealing on
682 the impact the surface modification exerted on catalyst properties. In these n-

683 heptane oxidations, **SiI-CI/MnPY** (**Y = 1, 2, 3**) catalysts showed chemoselectivity
684 for alcohols, whereas **SiO₂/MnPY** (**Y = 4, 5, 6**) catalysts promoted
685 chemoselectivity for carbonyl compounds (ketones and aldehyde).

686 Overall, **SiI-CI/MnP1** stood out as particularly resistant against oxidative
687 destruction and catalytically robust in cyclohexane, n-heptane, and adamantane
688 model-substrate oxidations, without significant loss of either efficiency or
689 selectivity for at least three oxidation cycles.

690

691

692 **Conflicts of interest**

693 There are no conflicts to declare.

694

695

696 **Acknowledgment**

697 We are gratefully thankful to Prof. Ynara M. Idemori for the access to her
698 laboratory facilities at Universidade Federal de Minas Gerais (Belo Horizonte,
699 MG, Brazil), where our first catalytic studies were carried out, and for her
700 continuous encouragement and stimulating discussions. We thank Dr. Ramon K.
701 S. Almeida (University of Campinas, Brazil) for the ¹³C and ²⁹Si NMR spectra.
702 Electron Microscopy Center at University Federal of Paraná (CME-UFPR, Brazil)
703 is gratefully acknowledged for SEM/TEM analyses. Financial support from
704 Conselho Nacional de Desenvolvimento Científico e Tecnológico (CNPq, Brazil),
705 Coordenação de Aperfeiçoamento de Pessoal de Nível Superior (CAPES,
706 Brazil), and Financiadora de Estudos e Projetos (FINEP, Brazil) is acknowledged.
707 V.H.A. Pinto thanks CAPES for a PhD scholarship. N.K.S.M. Falcão and B. Mariz-
708 Silva thank CNPq and CAPES, respectively, for MSc scholarships.

709

710 **References**

- 711 1 V.H.A. Pinto, J.S. Rebouças, G.M. Ucoski, E.H. Faria, B.F. Ferreira, R.A.S.S.
712 Gil, S. Nakagaki, *Appl. Catal., A*, 2016, **526**, 9.
- 713 2 G.M. Ucoski, V.H.A. Pinto, G. DeFreitas-Silva, J.S. Rebouças, R. Marcos Silva-
714 Jr., I. Mazzaro, F.S. Nunes, S. Nakagaki, *Microporous Mesoporous Mater.*,
715 2018, **265**, 84.
- 716 3 G.M. Ucoski, V.H.A. Pinto, G. DeFreitas-Silva, J.S. Rebouças, I. Mazzaro, F.S.
717 Nunes, S. Nakagaki, *ChemistrySelect*, 2017, **2**, 3703.
- 718 4 J.S. Rebouças, M.E.M.D. Carvalho, Y.M. Idemori, *J. Porphyrins*
719 *Phthalocyanines*, 2002, **6**, 50.
- 720 5 G.F. Silva, D.C. da Silva, A.S. Guimarães, E. do Nascimento, J.S. Rebouças,
721 M.P. de Araujo, M.E.M.D. de Carvalho, Y.M. Idemori, *J. Mol. Catal. A:*
722 *Chem.*, 2007, **266**, 274.
- 723 6 G.M. Ucoski, G.S. Machado, G. DeFreitas-Silva, F.S. Nunes, F. Wypych, S.
724 Nakagaki, *J. Mol. Catal. A: Chem.*, 2015, **408**, 123.
- 725 7 S. Nakagaki, G.K.B. Ferreira, Katia J. Ciuffi, A.L. Marcal, *Curr. Org. Synth.*,
726 2014, **11**, 67.
- 727 8 J.S. Rebouças, I. Spasojević, D.H. Tjahjono, A. Richaud, F. Méndez, L. Benov,
728 I. Batinić-Haberle, *Dalton Trans.* 2008, **9**, 1233.
- 729 9 I. Batinić-Haberle, J.S. Rebouças, L. Benov, I. Spasojevic. In *Handbook of*
730 *Porphyrin Science*, ed. K.M. Kadish, K.M. Smith, R. Guilard, World
731 Scientific Publishing Company, New York, 11, 2011, 52, 291-393.
- 732 10 A. Tovmasyan, C.G.C. Maia, T. Weitner, S. Carballal, R.S. Sampaio, D. Lieb,
733 R. Ghazaryan, I. Ivanovic-Burmazovic, G. Ferrer-Sueta, R. Radi, J.S.
734 Rebouças, I. Spasojevic, L. Benov, I. Batinić-Haberle, *Free Radic. Biol.*
735 *Med.*, 2015, **86**, 308.
- 736 11 V.H.A. Pinto, N.K.S.M. Falcão, J.C. Bueno-Janice, I. Spasojević, I. Batinić-
737 Haberle, J.S. Rebouças, In *Redox-Active Therapeutics*, ed. I. Batinić-
738 Haberle, J.S. Rebouças, I. Spasojević, Springer, Switzerland, 2016, 9,
739 213-243.
- 740 12 P. Battioni, J.P. Lallier, L. Barloy, D. Mansuy, *J. Chem. Soc., Chem. Commun.*,
741 1989, **01**, 1149.
- 742 13 Y. Iamamoto, Y. M. Idemori, S. Nakagaki, *J. Mol. Catal. A: Chem.*, 1995, **99**,

- 743 187.
- 744 14 H.S. Hilal, M.L. Sito, A.F. Schreiner, *Inorg. Chim. Acta*, 1991, **189**, 141.
- 745 15 H.S. Hilal, W. Jondi, S. Khalaf, A. Keilani, M. Suleiman, A.F. Schreiner, *J. Mol.*
746 *Catal. A: Chem.*, 1996, **113**, 35.
- 747 16 M.S. Saeedi, S. Tangestaninejad, M. Moghadam, V. Mirkhani, I.
748 Mohammadpoor-Baltork, A.R. Khosropour, *Polyhedron*, 2013, **49**, 158.
- 749 17 M. Moghadam, S. Tangestaninejad, M.H. Habibi, V. Mirkhani, *J. Mol. Catal.*
750 *A: Chem.*, 2004, **217**, 9.
- 751 18 M. Moghadam, S. Tangestaninejad, V. Mirkhani, I. Mohammadpoor-Baltork,
752 A.A. Abbasi-Larki, *Appl. Catal., A*, 2008, **349**, 177.
- 753 19 M. Moghadam, S. Tangestaninejad, V. Mirkhani, I. Mohammadpoor-baltork,
754 N. Sirjanian, S. Parand, *Bioorg. Med. Chem.*, 2009, **17**, 3394.
- 755 20 Q. Zhu, S. Maeno, R. Nishimoto, T. Miyamoto, M. Fukushima, *J. Mol. Catal.*
756 *A: Chem.*, 2014, **385**, 31.
- 757 21 A.M. Machado, F. Wypych, S.M. Drechsel, S. Nakagaki, *J. Colloid Interface*
758 *Sci.*, 2002, **254**, 158.
- 759 22 P.R. Cooke, J.R.L. Smith, *J. Chem. Soc., Perkin Trans. 1*, 1994, **14**, 1913.
- 760 23 F.S. Vinhado, C.M.C. Prado-manso, H.C. Sacco, Y. Iamamoto, *J. Mol. Catal.*
761 *A: Chem.*, 2001, **174**, 279.
- 762 24 J. Poltowicz, J. Poltowicz, E. Serwicka, E. Serwicka, E. Bastardo-Gonzalez,
763 E. Bastardo-Gonzalez, W. Jones, W. Jones, R. Mokaya, R. Mokaya, *Appl.*
764 *Catal., A*, 2001, **218**, 211.
- 765 25 G.M. Ucoski, F.S. Nunes, G. Defreitas-Silva, Y.M. Idemori, S. Nakagaki, *Appl.*
766 *Catal., A*, 2013, **459**, 121.
- 767 26 L. Barloy, P. Battioni, D. Mansuy, *J. Chem. Soc., Chem. Commun.* 1990, **0**,
768 1365.
- 769 27 U. Schuchardt, D. Cardoso, R. Sercheli, R. Pereira, R.S. da Cruz, M.C.
770 Guerreiro, D. Mandelli, E.V. Spinacé, E.L. Pires, *Appl. Catal., A*, 2001, **211**,
771 1.
- 772 28 A.M. Kirillov, M.V. Kirillova, A.J.L. Pombeiro, *Adv. Inorg. Chem.*, 2013, **65**, 1.
- 773 29 T.A. Fernandes, C.I.M. Santos, V. André, J. Kłak, M.V. Kirillova, A.M. Kirillov,
774 *Inorg. Chem.*, 2016, **55**, 125.
- 775 30 M.A. Andrade, L.M.D.R.S. Martins, *Catalysis*, 2020, **10**, 2.
- 776

- 777 31 Y. Wu, Z. Li, C. Xia, *Ind. Eng. Chem. Res.*, 2016, **55**, 1859.
- 778 32 V.L.S. Augusto Filha, O.G. da Silva, J.R. da Costa, A.F. Wanderley, M.G. da
779 Fonseca, L.N.H. Arakaki, *J. Therm. Anal. Calorim.*, 2007, **87**, 621.
- 780 33 F. Wang, Z. Zhang, J. Yang, L. Wang, Y. Lin, Y. Wei, *Fuel*, 2013, **107**, 394.
- 781 34 P. Zhang, J. Chen, L. Jia, *J. Chromatogr. A*, 2011, **1218**, 3459.
- 782 35 C.V. Santilli, N.L.D. Filho, S.H. Pulcinelli, J.C. Moreira, Y. Gushikem, *J. Mater.*
783 *Sci. Lett.*, 1996, **15**, 1450.
- 784 36 N.L.D. Filho, Y. Gushikem, E. Rodrigues, J.C. Moreira, W.L. Polito, *J. Chem.*
785 *Soc., Dalton Trans.*, 1994, **141**, 1493.
- 786 37 P. Worthington, P. Hambright, R.F.X. Williams, J. Reid, C. Burnham, A.
787 Shamim, J. Turay, D.M. Bell, R. Kirkland, R.G. Little, N. Datta-Gupta, U.
788 Eisner, *J. Inorg. Biochem.*, 1980, **12**, 281.
- 789 38 I. Batinić-Haberle, L. Benov, I. Spasojević, I. Fridovich, *J. Biol. Chem.*, 1998,
790 **273**, 24521.
- 791 39 I. Batinić-Haberle, I. Spasojevic, P. Hambright, L. Benov, A.L. Crumbliss, I.
792 Fridovich, *Inorg. Chem.*, 1999, **38**, 4011.
- 793 40 I. Batinić-Haberle, I. Spasojević, R.D. Stevens, P. Hambright, I. Fridovich, *J.*
794 *Chem. Soc., Dalton Trans.*, 2002, **13**, 2689.
- 795 41 A. Harriman, G. Porte, *J. Chem. Soc., Faraday Trans. 2*, 1979, **75**, 1532.
- 796 42 J.S. Reboucas, I. Spasojević, I. Batinić-Haberle, *J. Pharm. Biomed. Anal.*,
797 2008, **48**, 1046.
- 798 43 J.S. Reboucas, I. Kos, Z. Vujaskovic, I. Batinić-Haberle. *J. Pharm. Biomed.*
799 *Anal.*, 2009, **50**, 1088.
- 800 44 V.H.A. Pinto, D. CarvalhoDa-Silva, J.L.M.S. Santos, T. Weitner, M.G. Fonseca
801 M.I. Yoshida, Y.M. Idemori, I. Batinić-Haberle, J.S. Rebouças, *J. Pharm.*
802 *Biomed. Anal.*, 2013, **73**, 29.
- 803 45 G.A.M. Safar, Y.M. Idemori, D. CarvalhoDa-Silva, J.S. Rebouças, M.S.C.
804 Mazzoni, A. Righi, *Nanotechnology*, 2012, 23 (2012) 275504.
- 805 46 H. Saltzman, J.G. Sharefkin, *Org. Synth.*, 1963, **43**, 60.
- 806 47 H. Van Damme, M. Crespín, F. Obrecht, M.I. Cruz, J.J. Fripiat, *J. Colloid*
807 *Interface Sci.*, 1978, **66**, 43.
- 808 48 F. Bedioui, *Coord. Chem. Rev.*, 1995, **144**, 39.
- 809 49 A. Nodzevska, A. Wadolowska, M. Watkinson, *Coord. Chem. Rev.*, 2019,
810 **283**, 181.

- 811 50 M.C. White, J. Zhao, *J. Am. Chem. Soc.*, 2018, **140**, 13988.
- 812 51 P. Gandeepan, T. Muller, D. Zell, G. Cera, S. Warratz, L. Ackermann, *Chem.*
813 *Rev.*, 2019, **119**, 2192.
- 814 52 M. Kirillova, T.A. Fernandes, V. Andre, A.M. Kirillov, *Org. Biomol. Chem.*,
815 2019, **17**, 7706.
- 816 53 S.M. Chen, *J. Mol. Catal. A: Chem.*, 1996, **112**, 277.
- 817 54 M.A. Schiavon, Y. Iamamoto, O.R. Nascimento, M.D.D. Assis, *J. Mol. Catal.*
818 *A: Chem.*, 2001, **174**, 213.
- 819 55 J. Połtowicz, K. Pamin, L. Matachowski, E.M. Serwicka, R. Mokaya, Y. Xia, Z.
820 Olejniczak, *Catal. Today*, 2006, **114**, 287.
- 821 56 S. Alavi, H. Hosseini-Monfared, M. Siczek, *J. Mol. Catal. A: Chem.*, 2013, **377**,
822 16.
- 823 57 A. Farokhi, H.H. Monfared, *J. Catal.*, 2017, **352**, 229.
- 824 58 R. De Paula, I.C.M.S. Santos, M.M.Q. Simões, M.G.P.M.S. Neves, J.A.S.
825 Cavaleiro, *J. Mol. Catal. A: Chem.*, 2015, **404–405**, 156.
- 826 59 C. Gilmartin, J.R.L. Smith, *J. Chem. Soc., Perkin Trans. 2*, 1995, **0**, 243.
- 827 60 G.S. Machado, O.J. de Lima, K.J. Ciuffi, F. Wypych, S. Nakagaki, *Catal. Sci.*
828 *Technol.*, 2013, **3**, 1094.
- 829 61 J.R.L. Smith, Y. Iamamoto, F.S. Vinhado, *J. Mol. Catal. A: Chem.*, 2006, **252**
830 23.
- 831 62 J.P. Collman, A. S. Chien, T.A. Eberspacher, J.I. Brauman, *J. Am. Chem.*
832 *Soc.*, 2000, **122**, 11098.
- 833 63 H. J. Lucas, E. R. Kennedy, *Org. Synth.*, 1942, **22**, 72.
- 834 64 B. Meunier, *Chem. Rev.*, 1992, **92**, 1411.
- 835 65 G.R. Friedermann, M. Halma, K.A.D. de F. Castro, F.L. Benedito, F.G. Doro,
836 S.M. Drechsel, A.S. Mangrich, M. das D. Assis, S. Nakagaki, *Appl. Catal.,*
837 *A*, 2006, **308**, 172.
- 838 66 D. Dolphin, T. Wijesekera, in *Metalloporphyrins in Catalytic Oxidations*, ed.
839 R.A. Sheldon, Marcel Dekker, New York, 1994, 7, 193–293.
- 840 67 R.A. Sheldon, *Catal. Today*, 2015, **247**, 4.
- 841 68 J.H. Han, S. Yoo, S. Seo, J. Hong, K. Kim, C. Kim, *Dalton Trans.*, 2005, **0**,
842 402.
- 843 69 G.B. Shul'pin, G. Süss-Fink, L.S. Shul'pina, *J. Mol. Catal. A: Chem.*, 2001,
844 **170**, 17.

- 845 70 F.B. Zanardi, I.A. Barbosa, P.C. de Sousa Filho, L.D. Zanatta, D.L. da Silva,
846 O.A. Serra, Y. Iamamoto, *Microporous Mesoporous Mater.*, 2016, **219** 161.
- 847 71 M.J. Gunter, P. Turner, *Coord. Chem. Rev.*, 1991, **108**, 115.
- 848 72 E. do Nascimento, G.F. Silva, F.A. Caetano, M.A.M. Fernandes, D.C. da Silva,
849 M.E.M.D. de Carvalho, J.M. Pernaut, J.S. Rebouças, Y.M. Idemori, *J.*
850 *Inorg. Biochem.*, 2005, **99**, 1193.
- 851 73 G.B. Shul'pin, Y.N. Kozlov, L.S. Shu'pina, *Catalysts*, 2019, **9**, 1046.
- 852 74 P. Chandra, T. Ghosh, N. Choudhary, A. Mohammad, S.M. Mobin, *Coord.*
853 *Chem. Rev.*, 2020, **411**, 213241.
- 854 75 J.M. Hudzik, J.W. Bozzelli, J.M. Simmie, *J. Phys. Chem. A*, 2014, **118** 9364.
- 855 76 G.S. Machado, K.A.D. de F. Castro, O.J. Lima, E.J. Nassar, K.J. Ciuffi, S.
856 Nakagaki, *Colloids Surf., A*, 2009, **349**, 162.
- 857 77 S. Nakagaki, F.L. Benedito, F. Wypych, *J. Mol. Catal. A: Chem.*, 2004, **217**
858 121.
- 859 78 K.A.D. de F. Castro, A. Bail, P.B. Groszewicz, G.S. Machado, W.H. Schreiner,
860 F. Wypych, S. Nakagaki, *Appl. Catal., A*, 2010, **386**, 51.
- 861 79 V.S. da Silva, S. Nakagaki, G.M. Ucoski, Y.M. Idemori, G. DeFreitas-Silva,
862 *RSC Adv.*, 2015, **5**, 106589.
- 863 80 A.A. Guedes, J.R.L. Smith, O.R. Nascimento, D.F. Costa Guedes, M.D.D.
864 Assis, *J. Braz. Chem. Soc.*, 2005, **16**, 835.
- 865 81 F.C. Skrobot, I.L.V. Rosa, A.P.A. Marques, P.R. Martins, J. Rocha, A.A.
866 Valente, Y. Iamamoto, *J. Mol. Catal. A: Chem.*, 2005, **237**, 86.
- 867 82 Y. Shiota, N. Kihara, T. Kamachi, K. Yoshizawa, *J. Org. Chem.*, 2003, **68**,
868 3958.
- 869 83 K.S. Suslick, in *The Porphyrin Handbook*, ed. K.M. Kadish, K.M. Smith, R.
870 Guillard, Academic Press, 2000, 28, 41–63.
- 871 84 R.H. Crabtree, *J. Chem. Soc., Dalton Trans.* 2001, **17**, 2437.

